A peptide trivalent arsenical inhibits tumor angiogenesis by perturbing mitochondrial function in angiogenic endothelial cells

Anthony S. Don,[1,3] Oliver Kisker,[2,3] Pierre Dilda,[1] Neil Donoghue,[1] Xueyun Zhao,[1] Stephanie Decollogne,[1] Belinda Creighton,[1] Evelyn Flynn,[2] Judah Folkman,[2] and Philip J. Hogg[1,2,*]

[1]Centre for Vascular Research, University of New South Wales and Department of Haematology, Prince of Wales Hospital, Sydney, Australia
[2]Department of Surgical Research, Children's Hospital, Boston, Massachusetts 02115
[3]These authors contributed equally to this work.
*Correspondence: p.hogg@unsw.edu.au

Summary

Mitochondria are the powerhouse of the cell and their disruption leads to cell death. We have used a peptide trivalent arsenical, 4-(N-(S-glutathionylacetyl)amino) phenylarsenoxide (GSAO), to inactivate the adenine nucleotide translocator (ANT) that exchanges matrix ATP for cytosolic ADP across the inner mitochondrial membrane and is the key component of the mitochondrial permeability transition pore (MPTP). GSAO triggered Ca^{2+}-dependent MPTP opening by crosslinking Cys^{160} and Cys^{257} of ANT. GSAO treatment caused a concentration-dependent increase in superoxide levels, ATP depletion, mitochondrial depolarization, and apoptosis in proliferating, but not growth-quiescent, endothelial cells. Endothelial cell proliferation drives new blood vessel formation, or angiogenesis. GSAO inhibited angiogenesis in the chick chorioallantoic membrane and in solid tumors in mice. Consequently, GSAO inhibited tumor growth in mice with no apparent toxicity at efficacious doses.

Introduction

Mitochondria are the focal point for a variety of proapoptotic signals and play a key role in the control and execution of the apoptotic program (Green and Evan, 2002). Proapoptotic stimuli, mitochondrial Ca^{2+} overload, and oxidative stress promote the opening of a nonspecific pore that spans the inner and outer mitochondrial membranes, known as the mitochondrial permeability transition pore (MPTP) (Haworth and Hunter, 1979; Hunter and Haworth, 1979; Crompton, 1999; Halestrap et al., 2002). Opening of the MPTP is accompanied by equilibration of all small solutes ($<$1.5 kDa) across the inner mitochondrial membrane, leading to mitochondrial swelling and outer membrane rupture, collapse of the proton motive force, uncoupling of oxidative phosphorylation, and hydrolysis of ATP produced by glycolysis. Transient MPTP opening results in the release of cytochrome c and the apoptosis-inducing factor from the mitochondrial intermembrane space, which in turn activates the caspase cascade (Crompton, 1999). A physiological role for the MPTP in rapid dissipation of mitochondrial Ca^{2+} overload has also been suggested (Rizzuto et al., 2000).

The adenine nucleotide translocator (ANT) is a 30 kDa protein that spans the inner mitochondrial membrane and is central to the MPTP (LeQuoc and LeQuoc, 1988; Halestrap et al., 1997). Other mitochondrial proteins, including cyclophilin D, the voltage-dependent anion channel, the peripheral benzodiazepin receptor, and Bcl-2 family members interact with ANT and influence the MPTP (Crompton, 1999; Halestrap et al., 2002). Thiol oxidizing or alkylating agents are powerful activators of the mitochondrial permeability transition that act by modifying one or more of the three unpaired cysteines in the matrix side of ANT (Halestrap et al., 2002). For this reason, the small trivalent arsenical, phenylarsenoxide (PAO), is a potent activator of the pore (Lenartowicz et al., 1991; McStay et al., 2002). Inorganic arsenic also activates the pore (Larochette et al., 1999; Belzacq et al., 2001).

PAO reacts with two thiols in ANT (McStay et al., 2002) forming a stable cyclic dithioarsinite in which both sulfur atoms are complexed to arsenic (Adams et al., 1990). Trivalent arsenicals are selective for closely spaced dithiols, as the ring structures formed between trivalent arsenicals and dithiols are markedly more stable than the noncyclic products formed with

SIGNIFICANCE

This study describes a way of selectively inactivating mitochondria in proliferating endothelial cells both in vitro and in vivo. Specifically, mitochondria in angiogenic endothelial cells in tumors have been targeted, which resulted in inhibition of tumor angiogenesis and tumor growth. This has been achieved using a peptide trivalent arsenical that inactivates a key mitochondrial transport protein (the adenine nucleotide translocator), which leads to proliferation arrest and cell death. The rational targeting of a mitochondrial protein with a small synthetic molecule described herein points the way to future rational design of angiogenesis inhibitors and general anticancer agents that target proliferating cells by disrupting mitochondrial function.

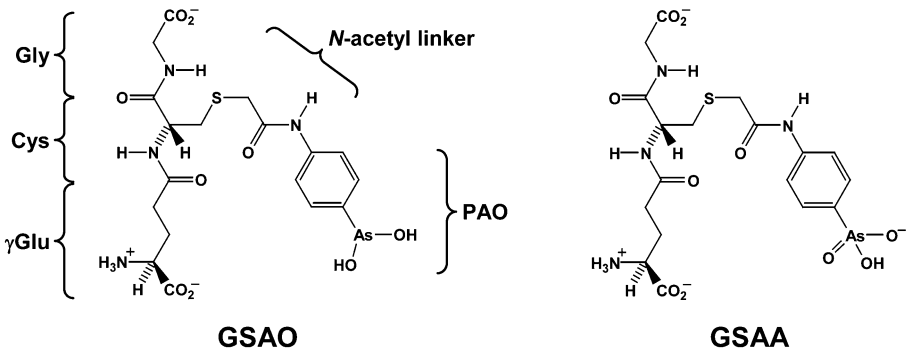

Figure 1. Structures of GSAO and GSAA

monothiols. PAO is lipophilic and is generally toxic for all cultured cells after exposure to nanomolar concentrations for 1 day (unpublished observations). We made a hydrophilic derivative of PAO by attaching it to the cysteine thiol of reduced glutathione (GlyCysγGlu) to produce 4-(N-(S-glutathionylacetyl)amino)phenylarsenoxide (GSAO) (Donoghue et al., 2000) (Figure 1). We now describe the induction of mitochondrial permeability by GSAO. The compound was toxic to proliferating, but not growth-quiescent, endothelial cells in vitro and an inhibitor of angiogenesis in vivo.

Results

GSAO induced the mitochondrial permeability transition

GSAO triggered swelling of isolated rat liver mitochondria in a time- and concentration-dependent manner (Figure 2Ai). The trivalent arsenical moiety of GSAO was responsible for this activity as the corresponding pentavalent arsenical (4-(N-((S-glutathionyl)acetyl)amino)benzenearsonic acid, GSAA) (Figure 1) had little effect on swelling (Figure 2Aii). Positive controls for pore opening were Ca^{2+} and phosphate (Pi) ions (Figure 2Ai) and PAO (Figure 2Aii).

ANT pore formation is controlled by the binding of Ca^{2+}, cyclophilin D, and adenine nucleotides under physiological conditions. The primary trigger for opening of the MPTP is a rise in matrix Ca^{2+} concentration. Chelation of Ca^{2+} with EGTA blocks pore opening, as does an excess of other divalent metal ions such as Mg^{2+} (Haworth and Hunter, 1979; Hunter and Haworth, 1979; Bernardi et al., 1992). Both EGTA and Mg^{2+} blocked GSAO-dependent swelling (Figure 2Aiii). Binding of cyclophilin D to ANT is necessary for pore opening at submillimolar Ca^{2+} concentrations. Cyclosporin A (CsA) blocks pore opening by binding to cyclophilin D and displacing it from ANT (Crompton et al., 1988; Halestrap et al., 2002). In addition, ADP and bonkrekic acid (BKA) inhibit pore opening by binding to ANT and decreasing the sensitivity of the trigger site to Ca^{2+} (Haworth and Hunter, 1979, 2000; Hunter and Haworth, 1979; LeQuoc and LeQuoc, 1988; Halestrap et al., 1997). CsA, ADP, and BKA all blocked the effect of GSAO on pore opening (Figure 2Aiii).

There is one cysteine in each of the three loops of ANT that protrude into the matrix, Cys^{57}, Cys^{160}, and Cys^{257}. The evidence indicates that PAO crosslinks Cys^{160} and Cys^{257} and enhances cyclophilin D binding while antagonizing ADP binding (McStay et al., 2002). The two effects together greatly sensitize the trigger site to Ca^{2+} concentration, which facilitates pore opening. In accordance with this mechanism, the time for half-maximal GSAO-mediated swelling of mitochondria decreased with increasing Ca^{2+} concentration (Figure 2B).

GSAO interacted directly with ANT

Considering that GSAO has the same dithiol reactivity as PAO, it was expected to mimic PAO's binding to ANT. Direct interaction of ANT with a biotin-tagged GSAO (4-(N-(S-(N-(6-((6-((biotinoyl)amino)hexanoyl)amino)hexanoyl)-glutathionyl)acetyl)amino) phenylarsenoxide, GSAO-B) is shown in Figures 2C and 2D.

Isolated mitochondria were incubated with 10 μM biotin-tagged GSAO (GSAO-B) or GSAA (GSAA-B), the labeled proteins were collected on avidin-coated beads, and the specifically bound proteins were eluted from the beads with an excess of the small synthetic dithiol, dithiothreitol. From comparison with the control experiment using GSAA-B, four GSAO-interacting proteins were clearly identified (Figure 2C). These proteins have molecular masses of ~60, 32, 30, and 19 kDa. The 30 kDa protein corresponded to ANT by Western blot (Figure 2D). Eosine-maleimide alkylates Cys^{160} in ANT and blocks ADP binding (Halestrap et al., 1997; Majima et al., 1998; McStay et al., 2002). GSAO competed for eosine-maleimide alkylation of ANT Cys^{160} (Figure 2E), which implied that GSAO, like PAO, crosslinks Cys^{160} and Cys^{257}.

GSAO localized to endothelial cell mitochondria

A striking feature of GSAO was that it rapidly localized to mitochondria in viable bovine aortic (BAE) (Figure 3) and human dermal microvascular (HMEC-1) (data not shown) endothelial cells. GSAO was conjugated to fluorescein (GSAO-F) and its subcellular localization was determined by confocal fluorescence microscopy. Mitochondrial staining was confirmed by colocalization of GSAO-F with the red-fluorescent Mitotracker probe, which accumulates in the mitochondria of actively respiring cells (Figure 3ii, 3iv, and 3vi) (Poot et al., 1996). The mitochondrial accumulation of GSAO-F was specific for the dithiol reactivity of GSAO as it was abolished in the presence of a 5-fold molar excess of dimercaptopropanol (Figure 3iii), and the corresponding pentavalent arsenical GSAA-F did not stain the cells (Figure 3v).

Endothelial cells were incubated with 3 μM tritiated GSAO or GSAA for 1, 2, or 3 days and the fmol of tritiated compound per cell was determined. The rate of uptake of GSAO was linear over the 3 days ($p < 0.05$) at 0.46 ± 0.02 fmol·cell^{-1}·day^{-1}, while for GSAA it was 0.35 ± 0.02 fmol·cell^{-1}·day^{-1}. The oxidation state of the arsenical moiety, therefore, had little effect on the rate of entry of the compound into endothelial cells. This

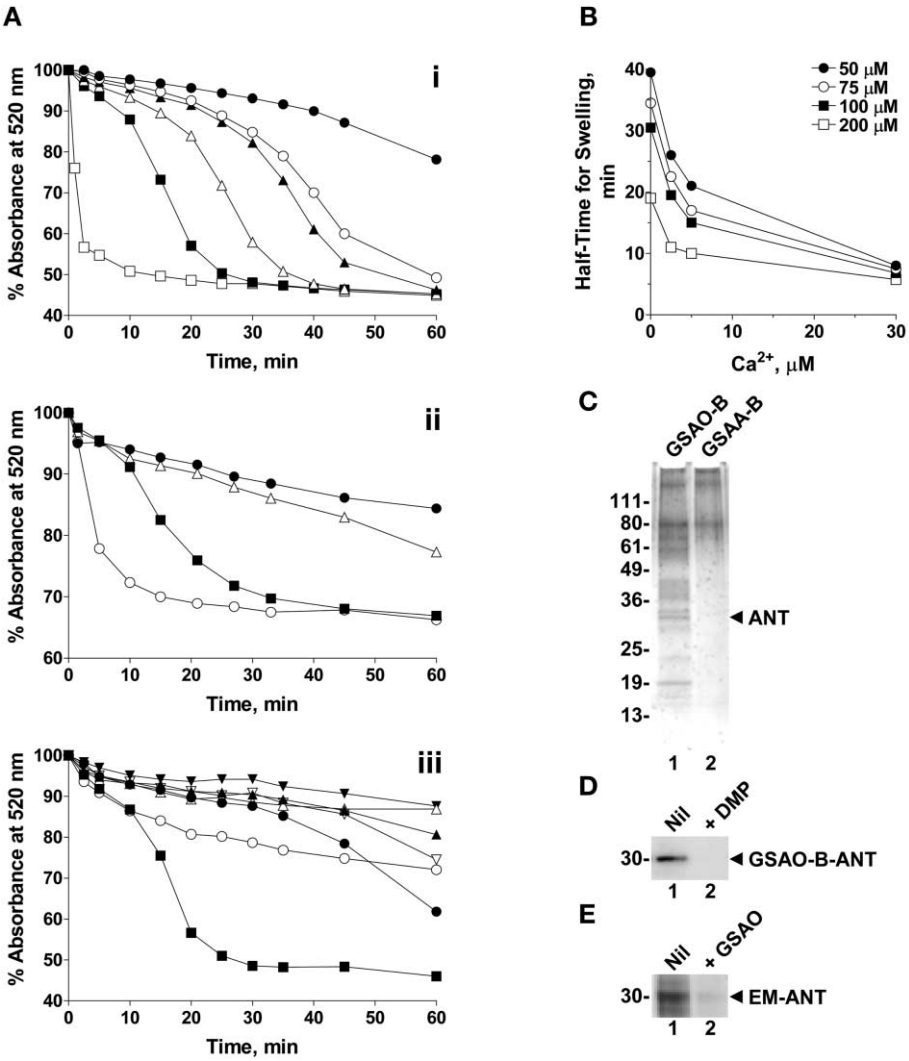

Figure 2. GSAO triggered MTP opening by binding to ANT

A: Mitochondrial swelling as measured by decrease in light scattering at 520 nm over 60 min. The traces are representative of a minimum of three experiments on at least two different mitochondrial preparations. Part (i): mitochondria were incubated with nil (●), 25 (○), 50 (▲), 100 (△), or 200 (■) μM GSAO, or 150 μM Ca^{2+} and 6 mM Pi (□). Part (ii): nil (●), 100 μM GSAA (△), 100 μM GSAO (■), or 25 μM PAO (○). Part (iii): mitochondria were incubated with 100 μM GSAO in the absence (■) or presence of 3 mM Mg^{2+} (▼), 100 μM EGTA (△), 10 μM BKA (▲), 5 μM CsA (▽), or 8 mM ADP (○). No treatment (●) shown for comparison.

B: Mitochondria were incubated with 50 (●), 75 (○), 100 (■), or 200 μM (□) GSAO at increasing Ca^{2+} concentrations and the time for half-maximal swelling was measured.

C: Mitochondria were incubated with 10 μM biotin-tagged GSAO or GSAA, the labeled proteins were collected on avidin-coated beads, and the specifically bound proteins were eluted from the beads with an excess of dithiothreitol. From comparison with the control experiment using GSAA-biotin (lane 2), four GSAO interacting proteins were identified with molecular masses of ~60, 32, 30, and 19 kDa (lane 1).

D: Western blot for ANT on mitochondrial proteins that bound to GSAO-B in the absence (lane 1) or presence (lane 2) of a 5-fold molar excess of 2,3-dimercaptopropanol (DMP).

E: SDS-PAGE of eosin-5-maleimide labeled ANT in the absence (lane 1) or presence (lane 2) of GSAO.

finding indicated that GSAA is a valid control compound for the intracellular effects of GSAO.

GSAO triggered mitochondrial depolarization and apoptosis in proliferating, but not growth-quiescent, endothelial cells

The finding that GSAO concentrated in the mitochondria of viable cells suggested that it might perturb mitochondrial function and cell viability. Mitochondrial Ca^{2+} uptake has been shown to occur concurrently with increases in cytosolic Ca^{2+} in response to physiological stimulants such as growth factors and G protein-coupled receptor agonists that are present in serum (Hoek et al., 1995; Crompton, 1999; Rizzuto et al., 2000). We anticipated, therefore, that proliferating (serum-stimulated) cells would be sensitized to GSAO-mediated MPTP opening compared to growth-quiescent (nonstimulated) cells because of the sharp dependence on Ca^{2+} for GSAO's effects on mitochondrial function (see Figure 2B). This would result in the selective induction of apoptosis in proliferating, but not growth-quiescent, cells. This theory was supported by the findings of Hoek et al. (1995), who observed that elevation of cytosolic Ca^{2+} leads to Ca^{2+} accumulation in mitochondria and an increase in PAO-induced mitochondrial swelling. The Ca^{2+} content of BAE cells incubated with 10% (proliferating) or 0.25% (growth-quiescent) serum and the effect of GSAO on the viability of these cells were measured.

Relative cellular Ca^{2+} concentrations were calculated with the ratiometric Ca^{2+} indicator dye Indo-1 and flow cytometry. The fluorescence ratio for Ca^{2+} bound to unbound Indo-1 was 48% higher in cells cultured for 48 hr in 10% serum compared to 0.25% serum and 22% higher in cells cultured for 24 hr. The Ca^{2+} content of proliferating endothelial cells was, therefore, significantly higher than in quiescent cells.

BAE cells were incubated for 48 hr in the presence of GSAO, and the number of cells remaining attached at the end of the treatment was measured. The IC_{50} for reduction in viability of proliferating BAE cells after 48 hr exposure to GSAO was ~75 μM (Figure 4Ai), whereas the compound had little effect on growth-quiescent cells. The same results were observed with HMEC-1 cells (data not shown). GSAA had no significant effect on cell number at concentrations up to 1.0 mM (data not shown). The effect of GSAO on proliferating cell viability was time dependent and a function of the cell density. The IC_{50} for GSAO decreased from ~75 μM to ~25 μM when the incubation time

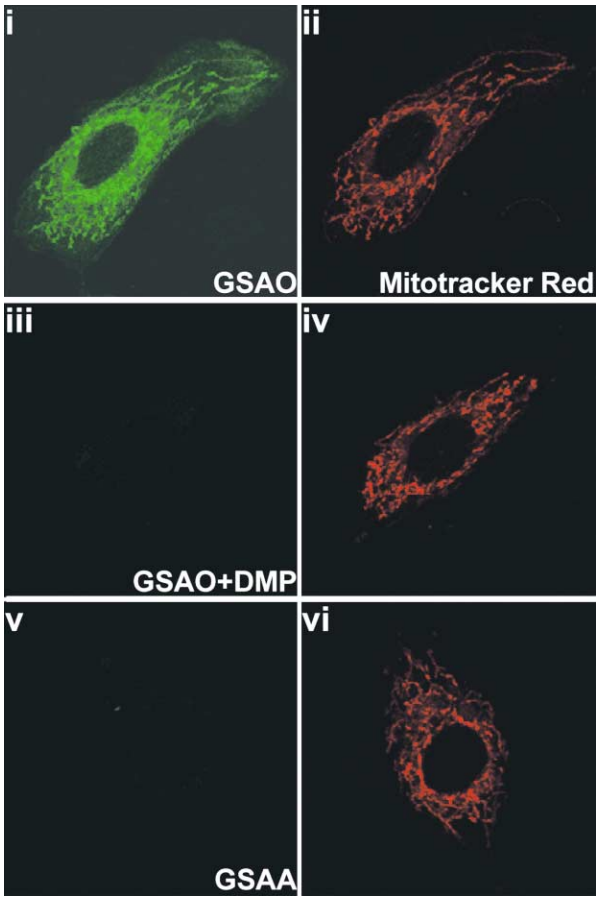

Figure 3. GSAO concentrated in mitochondria of viable cells

Confocal microscopy of BAE cells incubated with GSAO-F (i) and Mitotracker Red (ii) showing colocalization of the compounds in the mitochondria of a single cell. GSAO-F did not stain cells when incubated together with DMP (iii and iv). The pentavalent arsenical, GSAA-F, also did not stain cells (v and vi).

increased from 48 hr to 72 hr. The IC_{50} also decreased with decreasing cell density. PAO, in contrast, was equally toxic to both proliferating and growth-quiescent BAE cells with an IC_{50} of ~0.2 μM (Figure 4Aii).

Interestingly, there was a biphasic effect of PAO on endothelial cell viability. Low concentrations of PAO, but not GSAO, stimulated endothelial cell proliferation. Inorganic arsenic (arsenic trioxide) also has this effect on cell proliferation (Barchowsky et al., 1999). The glutathione pendant of GSAO, therefore, has changed the properties of the trivalent arsenical.

GSAO treatment induced caspase-3/7 activation (Figure 4B), loss of mitochondrial transmembrane potential, and surface presentation of phosphatidylserine (Figure 4C) in BAE cells. Mitochondrial transmembrane potential and phosphatidylserine exposure were measured using the JC-1 dye and FITC-conjugated annexin V, respectively. The ratio of distribution of JC-1 between the cytosol (green fluorescence) and mitochondria (red fluorescence) reflects mitochondrial transmembrane potential (Smiley et al., 1991). Caspase activation was commensurate with disruption of mitochondrial potential and exposure of phosphatidylserine. All three parameters increased with increasing GSAO concentration, indicating induction of apoptosis by GSAO.

GSAO inhibited ATP production and increased superoxide levels in proliferating, but not growth-quiescent, endothelial cells

The binding of GSAO to ANT and induction of apoptosis was expected to affect cellular ATP levels. The ATP content of proliferating BAE cells was approximately twice that of growth-quiescent cells, and incubation with 150 μM GSAO for 24 hr reduced ATP levels in proliferating cells by 30% (Figure 5Ai). To confirm that the decreased cellular ATP was due to an effect of GSAO on mitochondrial ATP synthesis rather than mitochondrial biogenesis, we measured mitochondrial mass using nonyl acridine orange. This dye binds to cardiolipin in the mitochondrial membrane (Petit et al., 1992). The mitochondrial mass of proliferating cells was approximately twice that of growth-quiescent cells and was unchanged by GSAO treatment (Figure 5Aii).

Reactive oxygen species, such as superoxide anion (O_2^-) and hydrogen peroxide (H_2O_2), are generated as a byproduct of respiration and play an important role as signaling intermediates in cellular proliferation, but at elevated concentrations, they arrest proliferation and induce apoptosis by damaging many cellular components (Raha and Robinson, 2000; Zanetti et al., 2001). One to two percent of oxygen consumed by mitochondrial respiration forms O_2^- through leakage of respiratory chain electrons directly to O_2 (Boveris et al., 1972; Turrens and Boveris, 1980). This leakage can derive from the NADH dehydrogenase (complex I), the succinate quinone dehydrogenase (complex II), or the cytochrome b-c1 reductase (complex III) of the respiratory chain (Papa, 1996; Turrens and Boveris, 1980; Raha and Robinson, 2000). Elevated O_2^- is also an indicator of mitochondrial damage or dysfunction (Fantin et al., 2002; Hiura et al., 2000). O_2^- is converted in the mitochondria to H_2O_2 by Mn superoxide dismutase (SOD), but can also be released from mitochondria through anion channels, where it is dismuted to H_2O_2 by cytosolic Cu/Zn SOD (Vanden Hoek et al., 1998).

BAE cells were treated for 24 hr with GSAO, and the cellular levels of O_2^- and H_2O_2 were measured using the dyes dihydroethidium and CM-H_2-DCFDA, respectively. Cellular levels of O_2^- increased linearly with GSAO concentration in proliferating, but not growth-quiescent, BAE cells (Figure 5B). Simultaneous analysis of cellular O_2^- and H_2O_2 levels using two channel flow cytometry indicated that this effect of GSAO was not due to an inhibition of SOD activity. O_2^- levels were increased in the majority of cells without a corresponding decrease in H_2O_2 (Figure 5C). There was no effect of GSAA on O_2^- or H_2O_2 levels (data not shown). The linear increase in O_2^- levels with GSAO treatment is consistent with a disruption of mitochondrial integrity. The elevated O_2^- likely contributes directly to the proliferation arrest and induction of apoptosis.

GSAO was selectively toxic towards endothelial cells compared to tumor cells

To distinguish between the antiproliferative and proapoptotic effects of GSAO, treated cells were stained with propidium iodide (PI) to detect late-apoptotic or dead cells. The total number of cells and the proportion of cells that were PI positive following 48 hr treatment with GSAO were measured by flow cytometry.

The IC_{50} for proliferation arrest of BAE (Figure 6A) or primary human dermal microvascular endothelial (Figure 6B) cells was

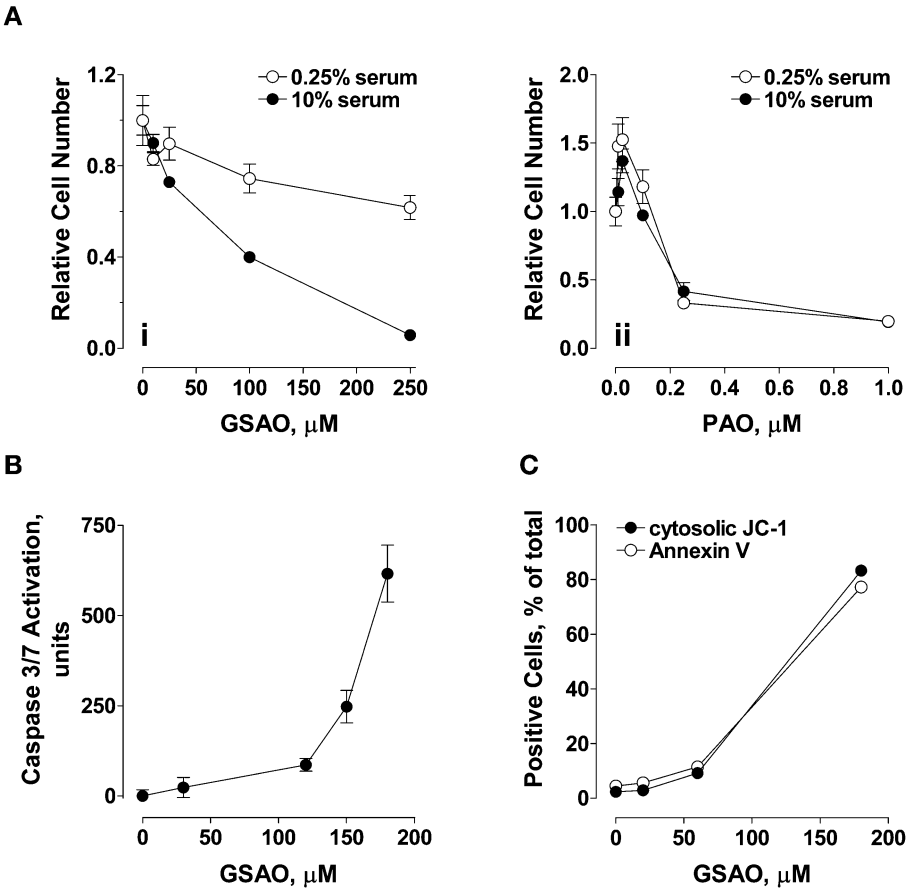

Figure 4. GSAO triggered mitochondrial depolarization and apoptosis in proliferating, but not growth-quiescent, endothelial cells

A: Number of attached BAE cells remaining after 48 hr incubation in medium containing 0.25% or 10% serum, with GSAO (i) or PAO (ii). Results are mean ± SEM of three experiments.

B: Activation of caspases 3/7 in BAE cells following 24 hr incubation with GSAO. Results are mean ± SEM of three experiments.

C: The percentage of cells positive for mitochondrial membrane depolarization (cytosolic JC-1) and annexin V binding following 24 hr incubation with GSAO. The same result was observed in two different experiments.

~10 μM and ~15 μM, respectively. The IC_{50} for loss of viability was ~75 μM and ~35 μM, respectively, indicating that GSAO arrested proliferation at lower concentrations than were necessary to induce apoptosis. The IC_{50} for proliferation arrest of bovine vascular smooth muscle cells was ~30 μM. In contrast, all tumor cells tested were more resistant to GSAO (Figures 6C–6G). The concentrations of GSAO that induce proliferation arrest and loss of viability are 3- to >32-fold and 2- to 9-fold higher, respectively, for tumor cells than for endothelial cells (Table 1). GSAO treatment caused Lewis lung carcinoma cells to disaggregate, which was the reason for the apparent increase in cell number for this tumor line (Figure 6E).

GSAO inhibited CAM angiogenesis

The ability of GSAO to selectively kill proliferating, but not growth-quiescent, endothelial cells in vitro suggested that it might be an effective inhibitor of angiogenesis in vivo. The sprouting of new capillaries from existing vessels is termed angiogenesis and is driven by proliferating endothelial cells (Carmeliet and Jain, 2000). In the normal adult mammal, angiogenesis is confined to the female reproductive cycle, wound healing, and diseases such as rheumatoid arthritis, psoriasis, diabetic retinopathy, and cancer. Tumor expansion and metastasis is dependent on tumor angiogenesis (Hanahan and Folkman, 1996).

The chick chorioallantoic membrane (CAM) assay has been used for the detection and analysis of angiogenesis inhibition (Nguyen et al., 1994). GSAO inhibited CAM angiogenesis (Figure 7A) in a concentration-dependent manner (Figure 7B). GSAA up to 50 μg per pellet had no effect on CAM angiogenesis. GSAO induces proliferation arrest in endothelial cells at 2.3- to 7.5-fold lower concentrations than are required to trigger apoptosis (see Figures 5A and 5B and Table 1). In the CAM assay, therefore, new blood vessels would not be expected to sprout from existing vessels in the vicinity of the GSAO pellet, which is what was observed. We next tested whether GSAO would inhibit tumor angiogenesis and tumor growth in mice.

GSAO inhibited tumor angiogenesis and tumor growth

Mice were administered GSAO by subcutaneous injection, and the plasma concentration of arsenic was measured by inductively coupled plasma mass spectrometry. This should reflect GSAO levels, as the concentration of arsenic in the plasma of untreated mice was below the level of detection. Subcutaneous administration of 10 mg/kg GSAO resulted in a plasma arsenic concentration of 6.4 ± 0.9 μM (n = 5) after 30 min, which is in the range of the IC_{50} for proliferation arrest of endothelial cells by GSAO in culture (Table 1). Plasma arsenic peaked at ≤30 min and returned to baseline after ~8 hr (Figure 7C).

The growth of established human and murine primary tumors in immunocompromised and immunocompetent mice, respectively, was suppressed by administration of GSAO. Treatment of SCID mice bearing ~0.1 g BxPC-3 (Figure 7D) or HT1080 (Figure 7E) tumors, or C57Bl6/J mice bearing ~0.1 g

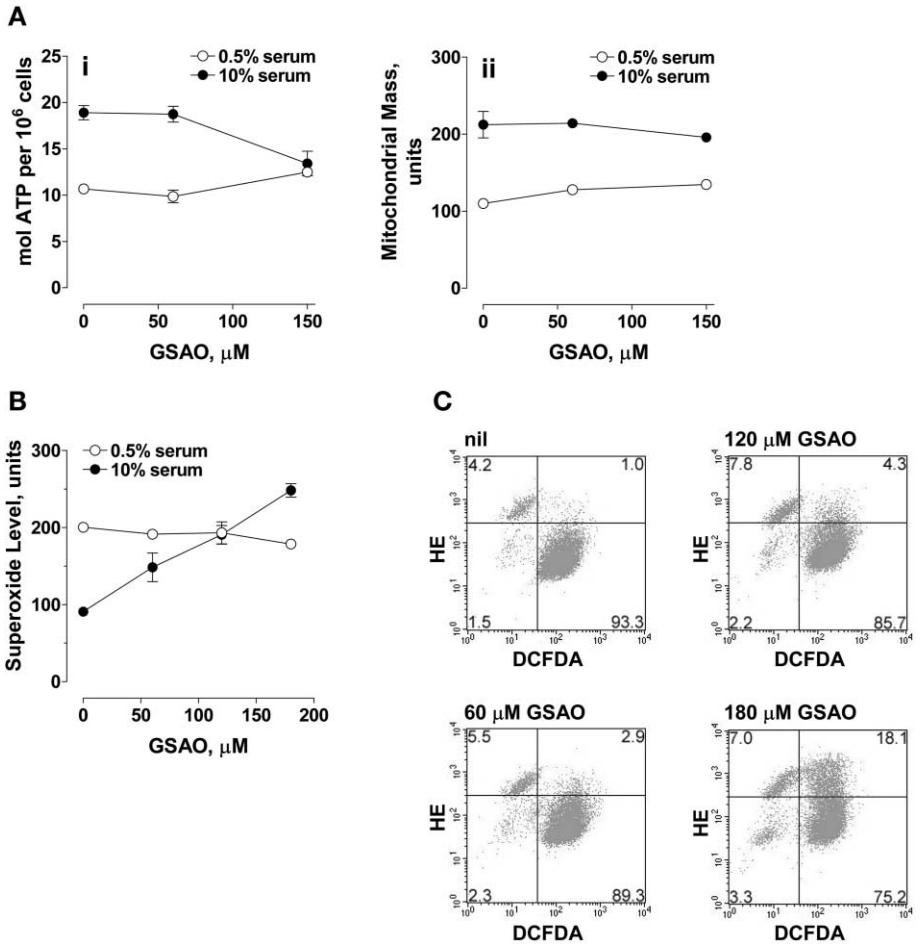

Figure 5. GSAO inhibited ATP production and increased superoxide levels in proliferating, but not growth-quiescent, endothelial cells

A: BAE cells were cultured for 24 hr in medium containing 0.5% or 10% serum and then for a further 24 hr in the presence of GSAO. In part i, cellular ATP levels were measured using a luciferin/luciferase assay. Results are mean ± SEM of four experiments. In part ii, mitochondrial mass was measured from uptake of nonyl acridine orange (NAO). Results are mean ± range of two experiments.

B: Superoxide level, measured with dihydroethidine, in BAE cells that had been cultured for 24 hr in medium containing 0.5% or 10% serum and then for a further 24 hr in the presence of GSAO. Results are mean ± range of two experiments.

C: Simultaneous measurement of O_2^- (*y* axis) and H_2O_2 (*x* axis) in BAE cells cultured in medium containing 10% serum and GSAO for 24 hr. Percentage of cells in each quadrant is shown in the outermost corner.

LLC tumors (Figure 7F), by subcutaneous administration of 10 mg/kg/day GSAO at a site remote from the tumor resulted in >90%, ~70%, and ~45% inhibition of the rate of tumor growth, respectively. Administration of control GSAA caused <20% inhibition of the rate of tumor growth in all experiments when compared to administration of vehicle alone (data not shown). This small inhibition of tumor growth by GSAA was perhaps due to enzymatic reduction of the compound to GSAO, possibly by a liver arsenate reductase (Radabaugh and Aposhian, 2000). There were no apparent adverse affects of administration of either GSAO or GSAA to either SCID or C57Bl6/J mice. The average mice weights of the GSAO and GSAA treatment groups over the course of the experiments were not significantly different (data not shown), and there were no macroscopic differences or morphological changes apparent in the heart, lungs, liver, kidneys, and spleen of GSAO- or GSAA-treated mice.

Immunohistochemical analysis of the tumors from the experiment described in Figure 7D indicated a significant reduction in blood vessel density in the GSAO-treated tumors ($p < 0.001$) (Figures 7G and 7H). The proliferative indices of the GSAA- and GSAO-treated tumors were the same, while there was a significant increase in the apoptotic indices of GSAO- versus GSAA-treated tumors ($p = 0.05$) (Figure 7H).

The effect of GSAO on tumor growth is consistent with inhibition of tumor angiogenesis. GSAO arrested proliferation of endothelial cells in vivo but had no effect on BxPC-3 proliferation at >30-fold higher concentrations (Table 1), and systemic administration of GSAO markedly reduced tumor vascularity in vivo but had no effect on the proliferative index of the BxPC-3 tumor cells (Figure 7H). There was a significant increase in apoptosis of the BxPC-3 tumor cells, which is in accordance with inhibition of tumor angiogenesis (O'Reilly et al., 1997). The high rate of apoptosis balances the high proliferative rate of the tumor cells, resulting in no net gain in tumor size (Holmgren et al., 1995).

Discussion

GSAO localized to endothelial cell mitochondria and induced Ca^{2+}-dependent opening of the MPTP in isolated mitochondria, directly crosslinking two cysteine residues on the matrix side of ANT. Perturbation of mitochondrial function in cultured endothelial cells was evidenced as an increase in the cellular levels of O_2^- at subapoptotic concentrations of GSAO, and a decrease in cellular ATP and loss of mitochondrial transmembrane potential at higher GSAO concentrations. High levels of reactive oxygen species can arrest proliferation and induce apoptosis by damaging lipids, proteins, DNA, and RNA (Raha and Robinson, 2000; Davis et al., 2001; Zanetti et al., 2001). In contrast, GSAO had little effect on mitochondrial function and viability of growth-quiescent endothelial cells.

Although we cannot exclude an effect of GSAO on the activ-

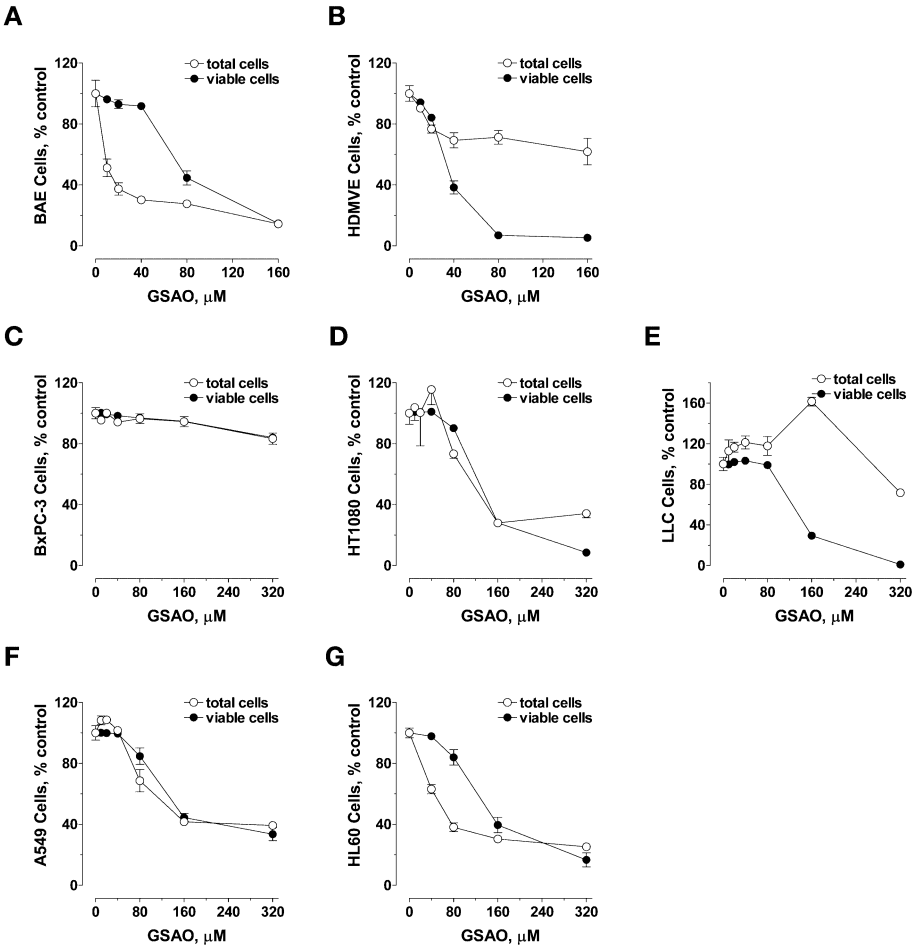

Figure 6. GSAO was selectively toxic towards endothelial cells compared to tumor cells

Effect of GSAO on cell proliferation and viability for two types of primary endothelial cell (**A** and **B**) and five tumor cell lines (**C**–**G**). Four human (BxPC-3 pancreatic, HT1080 fibrosarcoma, A549 lung, and HL60 erythroid leukaemia) and one murine (LLC lung) carcinoma cell lines were tested. Results are mean ± SEM of three treatments.

ity of other mitochondrial proteins, the mitochondrial swelling and cell-based assays point to ANT as the relevant target in terms of the consequences for endothelial cell proliferation and viability. ANT is the most abundant protein of the inner mitochondrial membrane (Klingenberg and Nelson, 1994), and it has been well established that disruption of ANT has major consequences for mitochondrial integrity and cell survival (Halestrap et al., 2002). Proving that ANT is the most relevant target for GSAO in endothelial cells using genetic approaches is problematic. Overexpression of ANT in mammalian cells induces apoptosis (Bauer et al., 1999) in a manner that may be unrelated to formation of the MPTP (Halestrap et al., 2002).

The strong selectivity of GSAO for proliferating cells was probably a consequence of two related events: the greater propensity for MPTP opening due to higher mitochondrial Ca^{2+} levels and the higher respiration rate in proliferating cells. The elevated cellular levels of O_2^- most likely resulted from uncontrolled production and/or release from mitochondria following opening of the MPTP by GSAO. GSAO treatment did not increase cellular H_2O_2 levels, which implied that it did not affect the thioredoxin and glutathione thiol buffering systems (Davis et al., 2001; Gladyshev et al., 2001; Chen et al., 2002). Depleting the cellular thiol buffering capacity would be expected to result in elevated H_2O_2 levels (Powis and Montfort, 2001).

Table 1. Effect of GSAO on proliferation and viability of endothelial and tumor cells

Cell type	Proliferation arrest IC_{50}, μM	Loss of viability IC_{50}, μM
BAE (bovine aortic endothelial)	10	75
HDMVE (human dermal endothelial)	15	35
BxPC-3 (human pancreatic carcinoma)	>320	>320
HT1080 (human fibrosarcoma)	95	130
LLC (murine lung carcinoma)	ND[a]	140
A549 (human lung carcinoma)	80	150
HL60 (human erythroid leukaemia)	50	140

[a] Not determined. LLC cells aggregate in culture and GSAO treatment caused the cells to disaggregate, which compromised the estimation of total cell number.

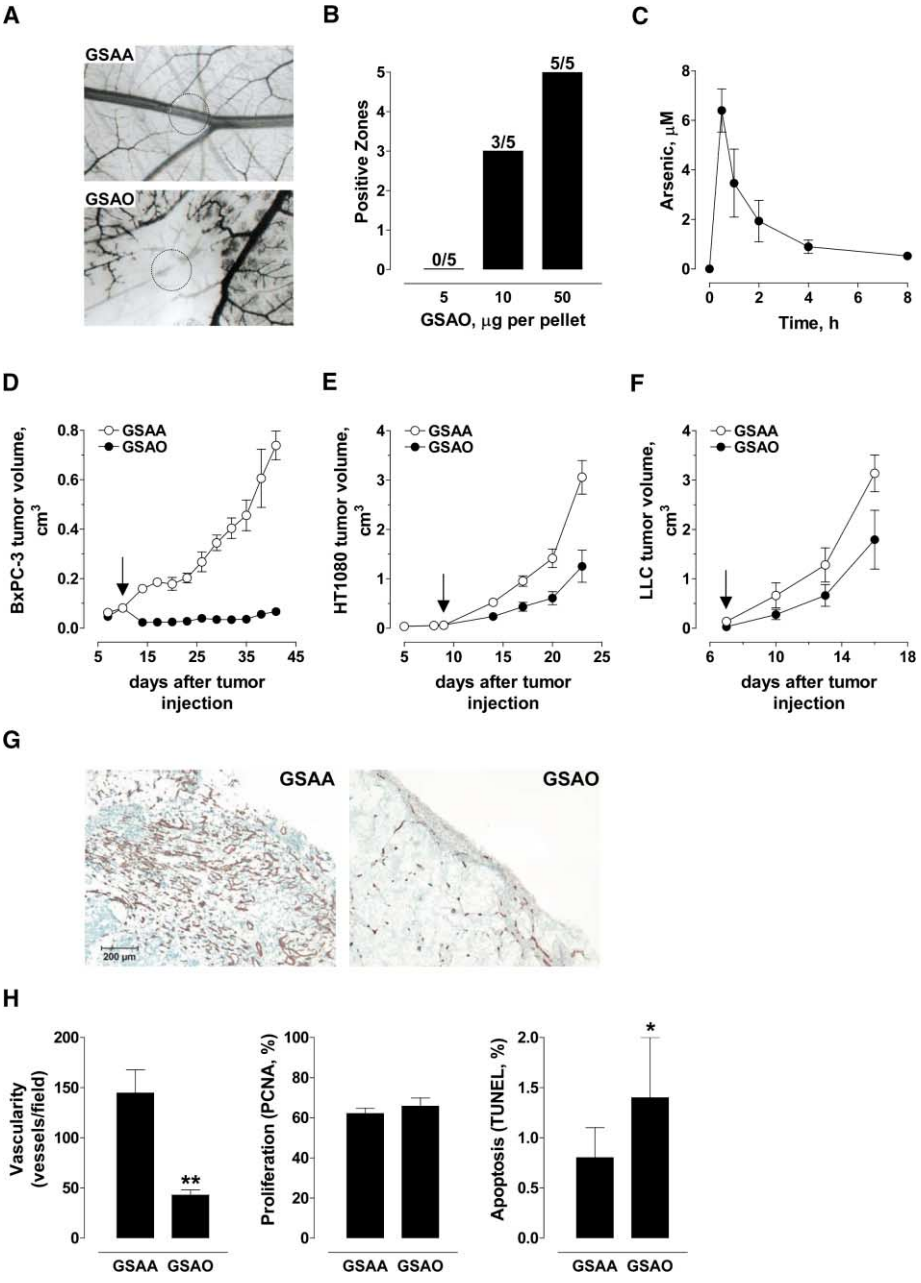

Figure 7. GSAO inhibited CAM and tumor angiogenesis

A: Photographs of CAM's after incubation with methylcellulose discs containing 10 μg of either GSAA (top) or GSAO (bottom) for 48 hr. The dotted circle indicates the placement of the disc.

B: The number out of 5 zones positive for angiogenesis inhibition at 5, 10, or 50 μg of GSAO per pellet. GSAA did not inhibit CAM angiogenesis up to 50 μg per pellet.

C: Plasma arsenic concentrations following subcutaneous administration of 10 mg/kg GSAO to Balb c mice. The data points are the mean ± SEM of 3–5 mice plasmas.

D–F SCID mice bearing ~0.1 g BxPC-3 (**D**) or HT1080 (**E**) tumors, or C57Bl6/J mice bearing ~0.1 g LLC tumors (**F**), were randomized into two groups (n = 4) and treated subcutaneously with either GSAA or GSAO at 10 mg/kg/day in 0.2 ml of PBS containing 100 mM glycine. The data points are the mean ± SEM of the tumor volumes. The arrows indicate start of treatment.

G–H Histological sections of the BxPC-3 tumors from the experiment shown in **D** at day 31 of treatment with GSAA or GSAO were analyzed for vascularity (CD31), proliferation (PCNA), and apoptosis (TUNEL). An example of the staining for CD31 is shown in **G**, and the quantitation of blood vessel density, tumor cell proliferation, or apoptosis is shown in **H**. The stars represent significant difference from control: ** is $p < 0.001$ while * is $p = 0.05$.

GSAO's accumulation in the mitochondria of viable endothelial cells was potentially driven by its interaction with ANT, which is abundant in the inner mitochondrial membrane. Sequestration of GSAO by mitochondrial dithiols, such as those in ANT, would drive further entropic import of GSAO into the matrix. This mechanism is supported by the finding that GSAA, which has effectively the same charge and size as GSAO, did not accumulate in mitochondria. Similarly, retention of the Mitotracker CMXRos dye is thought to be due to its reaction with mitochondrial protein thiols via its chloromethyl moiety (Poot et al., 1996).

Three isoforms of ANT have been described in mammalian cells, which are differentially expressed in various human tissues (Ku et al., 1990; Doerner et al., 1997). The ANT2 isoform is selectively expressed in proliferating cells together with the immediate-early genes (Battini et al., 1987). However, it seems unlikely that isoform specificity accounts for the selectivity of GSAO for proliferating cells, since the three isoforms share >95% sequence similarity and the two cysteines that react with GSAO, Cys^{160} and Cys^{257}, are conserved in all three. Furthermore, we have observed no obvious difference in GSAO's mitochondrial localisation in proliferating versus growth-quiescent endothelial cells by confocal microscopy or sub-cellular fractionation (data not shown).

The mechanism of the selectivity of GSAO for endothelial versus tumor cells is under investigation. Preliminary findings suggest that the selectivity may relate to the capacity of the cell to buffer GSAO's arsenical moiety. A major buffer appears to be reduced glutathione, as both endothelial and tumor cells are more susceptible to GSAO when pre-treated with the gluta-

thione synthesis inhibitor buthionine sulfoximine (data not shown). A role for cellular glutathione in buffering inorganic arsenic, for example, is well established (Ochi, 1997; Schuliga et al., 2002). Reduced numbers of mitochondria in tumor cells could also explain the selectivity. It has been known for some time that rapidly proliferating tumor cells have fewer mitochondria, lower levels of oxidative phosphorylation and elevated anaerobic glycolytic capacity (Pedersen, 1978; Papa, 1996).

Two other possible mechanisms for the anti-endothelial cell activity of GSAO were investigated. GSAO has been used to probe closely spaced protein thiols on the cell surface (Donoghue et al., 2000). However, prior blocking of all cell surface thiols with the hydrophilic thiol-alkylating agents 5,5′-dithiobis(2-nitrobenzoic acid) or 3-(N-maleimidylpropionyl)biocytin had no effect on the anti-endothelial cell activity of GSAO, indicating that GSAO's effects were not due to perturbation of a cell surface protein. Certain protein tyrosine phosphatases (PTPases) are inactivated by trivalent arsenicals, due to the presence of two unpaired cysteines in the active site (one of them is the catalytic cysteine) that form cyclic dithioarsinites with trivalent arsenicals (Liao et al., 1991; Defilippi et al., 1995; Yuan et al., 1998). Incubation of endothelial cells with high micromolar concentrations of GSAO resulted in increased tyrosine phosphorylation of two proteins (focal adhesion kinase and paxillin), and GSAO was found to inhibit two PTPases (PTP-PEST and PTP-1B). Overexpression of PTP-PEST or PTP-1B in endothelial cells did not blunt GSAO's effects on viability, however, which implied that these PTPases were not GSAO's primary target. Furthermore, inhibition of PTPase activity would be predicted to enhance endothelial proliferation and survival (Montesano et al., 1988). In fact, a PTP-1B inhibitor has recently been shown to promote neovascularization (Soeda et al., 2002).

GSAO inhibited tumor angiogenesis and tumor growth in mice with no apparent side effects. The safety of GSAO in mice may be due to its hydrophilicity, which limits its entry into cells and confines its distribution mostly to the intravascular compartment. Preliminary studies in mice have shown that GSAO is rapidly excreted in the urine within 30 min of intravenous administration and does not appear to accumulate in any organs.

Our findings indicate that hydrophilic dithiol-reactive compounds like GSAO appear to be an effective means of inhibiting endothelial cell proliferation and angiogenesis. A key aspect of this molecule is the glutathione pendant that safely delivers the arsenical warhead to endothelial cell mitochondria both in vitro and in vivo. The features of this pendant that permit delivery of the arsenical are currently being defined and refined.

Experimental procedures

Synthesis of GSAA

BRAA was prepared by a modification of the method described in Donoghue et al. (2000). p-Arsanilic acid (20.6 g, 95 mmol) was added in portions to a solution of sodium carbonate (20 g, 189 mmol) in water (200 ml). When all solids had dissolved, the solution was found to be pH 10 and was chilled at 4°C for 2 hr. Bromoacetyl bromide (15 ml, 173 mmol) in dry dichloromethane (35 ml) was added in two portions, each addition followed by vigorous shaking for 2 to 3 min. The mixture was allowed to stand for a few min, and the lower organic layer was drained off. 4-(N-(Bromoacetyl)amino)benzenearsonic acid (BRAA) was precipitated by acidification of the solution to about pH 2–3 with the dropwise addition of 98% sulfuric acid, collected by vacuum filtration and dried, giving BRAA as a white solid. BRAA (3.38 g, 10 mmol), reduced glutathione (3.23 g, 10.5 mmol), and sodium bicarbonate (3.15 g, 37.5 mmol) were mixed together, and the solid mixture was dissolved in portions in 0.5 M bicarbonate buffer (100 ml). The clear solution was found to be pH 9 and was thoroughly mixed and left overnight at room temperature. On the following day, the solution was acidified to neutral pH with the dropwise addition of 32% hydrochloric acid, and the product precipitated from absolute ethanol (1 liter) by dropwise addition of the acidified solution to the well-stirred alcohol. The mixture was stirred at room temperature for 1 hr and then left for 3 hr until the precipitate had settled. The clear ethanolic solution was decanted until ~300 ml were left, and then this was swirled and centrifuged at 2000 g for 5 min. The product 4-(N-((S-glutathionyl)acetyl) amino)benzenearsonic acid (GSAA) was washed by resuspension in fresh absolute ethanol and centrifuged again. The washing was repeated two more times, and the final suspension was dried to a white solid, GSAA, by rotary evaporation. The GSAA was characterized by ^{1}H-NMR (D_2O, 300 MHz) and ^{13}C-NMR (D_2O, 75 MHz) and has a molecular weight of 564.

Synthesis of GSAO

BRAA was prepared as described above and was then converted to 4-(N-(bromoacetyl)amino)benzenearsonous acid (BRAO) using the method described in Donoghue et al. (2000). The procedure for the conversion of BRAO to GSAO is a modification of that described in Donoghue et al. (2000), as follows. Reduced glutathione (16 g, 52 mmol) was dissolved in deoxygenated water (1 liter) under a nitrogen atmosphere (deoxygenated water was prepared by boiling followed by cooling to room temperature, all the time under an atmosphere of nitrogen). BRAO (25 g, 77 mmol) was suspended in the solution, and vigorous stirring of the mixture was applied until the undissolved BRAO had lost all tendency to float, at which point the rate of stirring was decreased. Triethylamine (16 ml, 11.6 g, 115 mmol) was added, and the mixture was stirred for at least 18 hr, all the time under nitrogen. Some colorless solid was removed by rapid vacuum filtration, and the filtrate was concentrated to a viscous gel on a rotary evaporator. The gel was diluted with ethanol (250 ml), the rate of stirring was increased, and then acetone (250 ml) was added, with formation of a white solid. After stirring for 2 hr under nitrogen, the solid was collected by vacuum filtration and dried at room temperature under vacuum to a constant weight. Analysis of the material by 1H-NMR allowed the amount of triethylamine to be determined. An equivalent amount of sodium hydroxide (i.e., 1 mmol NaOH per mmol triethylamine) was added in the form of a 10 M aqueous solution to a solution of the material in the minimum amount of deoxygenated water. The solution was stirred under nitrogen for 2 hr, and GSAO (as the sodium salt) was obtained by removal of the solvent on a rotary evaporator. The GSAO was characterized by the following methods: ^{1}H-NMR (D_2O, 400 MHz), ^{13}C-NMR (D_2O, 100 MHz), HPLC, and infrared spectroscopy (nujol mull). The elemental analysis was consistent with a composition of GSAO.2H_2O, and the mass spectrum gave the parent molecular ion at 549.1 min·u· $[GSAO+H]^{+}$. The purity of GSAO was >94% by HPLC.

Synthesis of biotin and fluorescein derivatives of GSAO and GSAA

GSAO-B was produced as described by Donoghue et al. (2000) and has a molecular weight of 1001. A solution of fluorescein-5-EX succinimidyl ester (Molecular Probes, Eugene, Oregon) (2.4 mg, 4.1 μmol) in DMSO (240 μl) was added to GSAO or GSAA (33.8 mM) in Mes buffer, pH 5.5 (5 mM, 473 μl), the mixture was diluted with bicarbonate buffer, pH 9 (0.5 M, 3.287 ml) and allowed to stand at room temperature for 80 min. The reaction was then diluted with glycine (100 mM) in phosphate-buffered saline (PBS) (4 ml) and allowed to stand at room temperature overnight. The final solution contained trivalent arsenical (2 mM) and glycine (50 mM). The molar ratio of fluorescein-5X to GSAO or GSAA was ~1.5:1. The molecular weights of GSAO- and GSAA-fluorescein (GSAO-F and GSAA-F) are 1024 and 1040, respectively.

Assay of arsenical concentration

The concentrations of GSAO, GSAO-B, and GSAO-F were measured by titrating with dimercaptopropanol and calculating the remaining free thiols with 5,5′-dithiobis(2-nitrobenzoic acid) (Sigma, St. Louis, Missouri) (Donoghue et al., 2000). The conjugates were sterile filtered and stored at 4°C in the dark until use. There was no significant loss in the active concentration of stock solutions of the arsenicals for at least a month when stored under these conditions. All GSAO and GSAA solutions used for experiments were dissolved in PBS containing 100 mM glycine. The glycine slows the oxidation of GSAO to GSAA (Donoghue et al., 2000).

Mitochondrial swelling assay
Mitochondria were isolated from the livers of ~250 g male Wistar rats using differential centrifugation as described previously (Schnaitman and Greenawalt, 1968). The final mitochondrial pellet was resuspended in 3 mM HEPES-KOH, pH 7.0 buffer containing 213 mM mannitol, 71 mM sucrose, and 10 mM sodium succinate at a concentration of 30 mg of protein per ml. Mitochondrial permeability transition induction was assessed spectrophotometrically by suspending the liver mitochondria at 0.5 mg of protein per ml at 25°C in 3 mM HEPES-KOH, pH 7.0 buffer containing 75 mM mannitol, 250 mM sucrose, 10 mM sodium succinate, and 2 μM rotenone. Swelling was measured by monitoring the associated decrease in light scattering at 520 nm using a Molecular Devices Thermomax Plus (Palo Alto, California) microplate reader. All reagents were purchased from Sigma.

Detection of mitochondrial proteins that bind GSAO
Rat liver mitochondria were suspended at 1 mg protein per ml in 3 mM HEPES-KOH, pH 7.0 buffer containing 213 mM mannitol, 71 mM sucrose, and 10 mM sodium succinate and incubated with 10 μM GSAO-B or GSAA-B for 1 hr at room temperature on a rotating wheel. The mitochondria were washed once with buffer, then sonicated in 0.3 ml ice-cold 25 mM Tris, pH 7.4 buffer containing 140 mM NaCl, 2.7 mM KCl, 0.5% Triton X-100, 0.05% Tween-20, 3 M Urea, 10 μM leupeptin, 1 μM aprotinin, 50 $\mu g.ml^{-1}$ 4-2-(aminoethyl)-benzene sulfonyl fluoride and 5 mM EDTA. Lysate was clarified by centrifugation at 18000 g for 10 min at 4°C and incubated with 30 μl of streptavidin-dynabeads (Dynal, Oslo, Norway) for 2 hr at 4°C to isolate the biotin-labeled proteins. The beads were washed twice with sonication buffer and twice with 25 mM Tris buffer containing 140 mM NaCl and 0.5% Triton X-100. Proteins bound specifically to GSAO's arsenical moiety were eluted from the beads by incubation with 40 μl of 25 mM Tris buffer containing 50 mM dithiothreitol for 5 min (Donoghue et al., 2000). The eluted proteins were resolved on 8%–16% gradient iGels (Gradipore, Sydney, Australia) under reducing conditions and silver stained.

Binding of GSAO to ANT
Rat liver mitochondria were prepared as described above and incubated with 10 μM GSAO-B in the absence or presence of 50 μM 2,3-dimercaptopropanol (Fluka, Buchs, SG, Switzerland). The GSAO-B labeled proteins were collected as described above, resolved on 8%–16% gradient iGels under reducing conditions, and transferred to PVDF membrane. Proteins were detected by Western blot using a 1:500 dilution of goat anti-human ANT polyclonal antibody (Santa Cruz Biotechnology, Santa Cruz, California) and 1:2000 dilution of rabbit anti-goat peroxidase-conjugated antibodies (Dako, Carpinteria, California).

Labeling of ANT with eosin-5-maleimide
Rat liver submitochondrial particles were prepared by sonication and differential centrifugation according to Majima et al. (1998). The particles were suspended at 20 mg of protein per ml in 10 mM Tris, pH 7.2 buffer containing 250 mM sucrose and 0.2 mM EDTA and incubated without or with 200 nmol GSAO per mg of protein for 10 min at 25°C, followed by 20 nmol of eosin-5-maleimide per mg of protein for 1 min at 0°C in the dark. The labeling was terminated by addition of 10 mmol of dithiothreitol per mg of protein. The proteins were resolved on 4%–20% gradient iGels and the eosin-labeled ANT was visualized by UV transillumination using a Fluor-S™ MultiImager (Bio-Rad, Hercules, California).

Cell culture
BAE cells were from Cell Applications, San Diego, California and BxPC-3, HT1080, LLC, A549, and HL60 cells were from ATCC, Bethesda, Maryland. BAE, HT1080, and LLC cells were cultured in DMEM, BxPC-3 cells in RPMI medium, A549 cells in F-12K medium, HL60 cells in IMDM, and HMEC-1 cells (Ades et al., 1992) in MCDB131 medium. The cells were supplemented with 10% fetal calf serum (FBS), 2 mM L-glutamine, and 1 $U \cdot ml^{-1}$ penicillin/streptomycin. HDMVE cells were a gift from Dr. Chris Jackson (Jackson et al., 1990) and cultured in MCDB131 supplemented with 20% human serum, 50 $\mu g \cdot ml^{-1}$ endothelial cell growth supplement, 50 $\mu g \cdot ml^{-1}$ heparin, 10 $ng \cdot ml^{-1}$ epidermal growth factor, and 1 $\mu g \cdot ml^{-1}$ hydrocortisone. Cell culture plasticware was from Techno Plastic Products (Trasadingen, Switzerland). Epidermal growth factor, hydrocortisone, and heparin were from Sigma. All other cell culture reagents were from Gibco (Gaithersburg, Maryland).

Immunocytochemistry and confocal microscopy
BAE cells were seeded at a density of 10^4 cells per well into 8-well Labtek glass chamber slides (Nunc, Naperville, Illinois) and allowed to adhere overnight. The cells were then incubated for 1 hr with 50 μM GSAO-F, 50 μM GSAO-F and 250 μM dimercaptopropanol, or 50 μM GSAA-F. All cells were counterstained with 100 nM MitotrackerTM Red CMXRos (Molecular Probes). The cells were then washed three times with serum-free medium and fixed for 10 min with 80% acetone and 20% methanol. Slides were mounted in VectaShield antifade agent (Vector Laboratories, Burlingame, California) and sealed with nail polish. Images were captured using a Leica DM IRB inverted microscope and confocal system, with Leica confocal software.

Cellular uptake assay
GSAO or GSAA was synthesized using tritiated glutathione (Amersham Biosciences, Buckinghamshire, United Kingdom). HMEC-1 cells were seeded at a density of 5×10^5 cells per well in 6-well culture plates and allowed to attach overnight. Cells were incubated with 3 μM tritiated GSAO or GSAA in the presence of 100 μM unlabeled reduced glutathione. The medium was removed and the cells were washed twice with PBS, detached with 20 mM EDTA/PBS, washed once with PBS, and solubilized with 100 μl of 20 mM Tris, pH 7.4 buffer containing 0.14 M NaCl, 1% Triton X-100, 0.5% sodium deoxycholate, 0.1% SDS, 2 mM EGTA, 50 $\mu g \cdot ml^{-1}$ AEBSF, 10 $\mu g \cdot ml^{-1}$ leupeptin, 1.0 μM aprotinin, and 1 $\mu g \cdot ml^{-1}$ pepstatin A. Samples were mixed with 5 ml aqueous scintillant ACSII (Amersham Pharmacia, Uppsala, Sweden) and counted for 4 min. Results were the mean ± standard error of triplicate cell treatments.

Cellular Ca^{2+} assay
BAE cells were seeded at 10^5 cells per well into 12-well plates in medium containing 10% serum, allowed to adhere overnight, then cultured for 24 or 48 hr in medium containing 10% or 0.25% serum. The cells were washed with PBS, incubated for 30 min in PBS containing 0.2% BSA and 2.5 μM Indo-1 (Sigma), washed once, then incubated for 60 min in medium containing 0.25% or 10% serum. The cells were detached with trypsin/EDTA, washed once to remove trypsin, resuspended in growth medium, and transferred to ice. Fluorescence was measured immediately using excitation at 350 nm and 510/20 nm (Ca^{2+} bound) and 440/40 nm (Ca^{2+}-free) emission filters. The ratio of violet/blue fluorescence was used to determine the relative intracellular Ca^{2+} concentration.

Cell proliferation and viability assays
To assay cell number with methylene blue, BAE cells were seeded at a density of 10^4 cells per well into 96-well plates and allowed to adhere overnight. Cells were arrested for 24 hr in medium containing 0.25% serum and cultured for a further 48 hr in medium containing 0.25% or 10% serum, in the presence of GSAO or PAO. Attached cells remaining after treatments were measured using methylene blue (Oliver et al., 1989). The anti-proliferative and cytotoxic effects of GSAO were assayed by flow cytometry with propidium iodide. Endothelial and tumor cells were seeded at a density of 5×10^4 cells per well into 12-well plates, allowed to adhere overnight, then treated for 48 hr with GSAO. Adherent cells were detached with trypsin/EDTA and combined with the growth medium containing the cells that had detached during treatment. The combined cells were pelleted, resuspended in 0.5 ml serum-free medium containing 1 $\mu g \cdot ml^{-1}$ propidium iodide (PI) (Molecular Probes), and analyzed by flow cytometry. The number of viable cells in the untreated control was normalized to 100%, and viability for all GSAO treatments was expressed as a percentage of control.

ATP assay
BAE cells in 6-well culture plates were arrested for 24 hr in 0.5% serum or left in 10% serum, then treated for 24 hr with GSAO. The cells were washed once then resuspended in 0.4 ml PBS containing 0.2% bovine serum albumin. A 50 μl sample of cells was mixed with 50 μl water and 100 μl ATP releasing agent and ATP concentration was measured using a luciferin/luciferase ATP assay mix (Sigma). Light units were converted to ATP concentrations using an ATP standard in place of the 50 μl water. Cell number was counted using a Beckman Coulter Counter and mol of ATP was expressed per million cells.

Caspase activation assay
BAE cells were seeded at a density of 10^4 cells per well in a 96-well plate and allowed to adhere overnight. The cells were incubated with increasing concentrations of GSAO for 24 hr and caspase-3/7 activity was determined using the APO-ONE™ Homogeneous Caspase-3/7 Assay (Promega, Madison, Wisconsin).

Superoxide, mitochondrial membrane potential, mitochondrial mass, and apoptosis assays
Proliferating or growth-quiescent BAE cells were treated for 24 hr with GSAO in 6-well culture plates, then detached with trypsin/EDTA, washed once, and resuspended at 2×10^6 cells per ml in serum-free medium. Cells were incubated for 30 min at room temperature with 0.5 $\mu g \cdot ml^{-1}$ JC-1, 50 $\mu l \cdot ml^{-1}$ annexin V-FITC, or 5 μM acridine orange 10-nonyl bromide (NAC), then washed once, resuspended in 0.5 ml serum-free medium, transferred to ice, and fluorescence was quantitated immediately by flow cytometry. To measure superoxide and hydrogen peroxide, the cells were incubated for 15 min at room temperature with 5 μM dihydroethidine (HE) and 5 μM CM-H_2-DCFDA in 0.5 ml serum-free medium, then immediately assessed by flow cytometry. JC-1, NAC, HE, CM-H_2-DCFDA were from Molecular Probes. Annexin V was from Pharmingen (La Jolla, California).

CAM assay
Fertilized 3-day-old white Leghorn eggs (Spafas, Norwich, Connecticut) were cracked, the embryos with intact yolks placed in 20×100 mm petri dishes and incubated for 3 days at 37°C and 3% CO_2 (Folkman, 1985). Methylcellulose (Fisher Scientific, Fair Lawn, New Jersey) discs containing 5, 10, or 50 μg of either GSAA or GSAO were then applied to the CAM of individual embryos and incubated for 48 hr at 37°C and 3% CO_2. The discs were made by desiccation of GSAA or GSAO in 10 μl of 0.45% methycellulose on teflon rods. The CAMs were observed using a stereomicroscope and scored for no obvious affect or inhibition of CAM angiogenesis as defined by avascular zones. On some occasions CAM blood vessels were injected with India ink and photographed.

Measurement of plasma arsenic
Female 7- to 9-week-old Balb c mice (University of New South Wales, Sydney, NSW) were administered 10 mg/kg GSAO in 0.2 ml of PBS containing 100 mM glycine by subcutaneous injection in the flank. Blood was collected by cardiac puncture into 50% acid citrate dextrose at discreet time intervals and plasma was prepared. The plasma samples were diluted ~5-fold with 70% w/w nitric acid to give 1 ml total solution. Small amounts of solid in the samples were dissolved by incubating at 56°C for 2.5 hr, before diluting 20-fold with water. The samples were then analyzed for arsenic using a Elan 6100 Inductively Coupled Plasma Mass Spectrometer (Perkin Elmer Sciex Instruments, Shelton, Connecticut).

Primary tumor growth assays
Female 7- to 9-week-old SCID or C57Bl6/J mice were used (Massachusetts General Hospital, Boston, Massachusetts). Mice were held in groups of 3 to 5 at a 12 hr day and night cycle and were given animal chow and water ad libidum. SCID or C57Bl6/J mice were anesthetized by inhalation of isoflurane, the dorsal skin shaved and cleaned with ethanol, and a suspension of 2.5×10^6 BxPC-3, HT1080, or LLC cells in 0.2 ml of PBS, or saline for LLC cells, was injected subcutaneously in the proximal midline. LLC cells were prepared according to O'Reilly et al. (1997). Tumors were allowed to establish and grow to a size of ~0.1 cm^3 after which they were randomized into two groups. Tumor volume was calculated using the relationship, $a \cdot b^2.0.52$, where a is the longest diameter and b the shortest. Animals were treated with either GSAA or GSAO at a dose 10 mg/kg/day in 0.2 ml of PBS containing 100 mM glycine. The compounds were administered subcutaneously at a site distant from the tumor. Tumor volume and animal weight were measured every 3 days. The tumors were excised and weighed when the animals were sacrificed.

Immunohistochemistry
Excised tumors were fixed in Buffered Formalde-Fresh (Fisher Scientific), embedded in paraffin, and 5 μm thick sections were cut and placed on glass slides. Sections were stained with haematoxylin and eosin or for CD31, PCNA (O'Reilly et al., 1997) or fragmented DNA (Gavrieli et al., 1992). Microvessels were counted in three tumors, including the smallest and largest, from the control and treatment groups, and the density was graded in the most active areas of neovascularization according to Weidner et al. (1991). The proliferative index was estimated by the percentage of cells scored under 400× magnification. A minimum of 1000 cells was counted in 3–5 sections. The apoptotic index was estimated by the percentage of cells scored under 400× magnification. A minimum of 15000 cells was counted in 12–15 sections.

Acknowledgments

This study was supported by NIH grant RO1-CA64481 and grants from the National Health and Medical Research Council of Australia, the New South Wales Cancer Council, and an infrastructure grant from the NSW Health Department. The technical assistance of Geraldine Jackson, Daniella Prox, Christian Becker, Angelina Lay, and Patricia Yam is acknowledged and we thank Janet Keast for providing the rat livers.

Received: January 9, 2003
Revised: April 24, 2003
Published: May 19, 2003

References

Adams, E., Jeter, D., Cordes, A.W., and Kolis, J.W. (1990). Chemistry of organometalloid complexes with potential antidotes: structure of an organoarsenic(III) dithiolate ring. Inorg. Chem. *29*, 1500–1503.

Ades, E.W., Candal, F.J., Swerlick, R.A., George, V.G., Summers, S., Bosse, D.C., and Lawley, T.J. (1992). HMEC-1: Establishment of an immortalized human microvascular endothelial cell line. J. Invest. Dermatol. *99*, 683–690.

Barchowsky, A., Roussel, R.R., Klei, L.R., James, P.E., Ganju, N., Smith, K.R., and Dudek, E.J. (1999). Low levels of arsenic trioxide stimulate proliferative signals in primary vascular cells without activating stress effector pathways. Toxicol. Appl. Pharmacol. *159*, 65–75.

Battini, R., Ferrari, S., Kaczmarek, L., Calabretta, B., Chen, S.T., and Baserga, R. (1987). Molecular cloning of a cDNA for a human ADP/ATP carrier which is growth-regulated. J. Biol. Chem. *262*, 4355–4359.

Bauer, M.K., Schubert, A., Rocks, O., and Grimm, S. (1999). Adenine nucleotide translocase-1, a component of the permeability transition pore, can dominantly induce apoptosis. J. Cell Biol. *147*, 1493–1502.

Belzacq, A.S., El Hamel, C., Vieira, H.L., Cohen, I., Haouzi, D., Metivier, D., Marchetti, P., Brenner, C., and Kroemer, G. (2001). Adenine nucleotide translocator mediates the mitochondrial membrane permeabilization induced by lonidamine, arsenite and CD437. Oncogene *20*, 7579–7587.

Bernardi, P., Vassanelli, S., Veronese, P., Colonna, R., Szabo, I., and Zoratti, M. (1992). Modulation of the mitochondrial permeability transition pore—effect of protons and divalent cations. J. Biol. Chem. *267*, 2934–2939.

Boveris, A., Oshino, N., and Chance, B. (1972). The mitochondrial production of hydrogen peroxide. Biochem. J. *128*, 617–630.

Carmeliet, P., and Jain, R.K. (2000). Angiogenesis in cancer and other diseases. Nature *407*, 249–257.

Chen, Y., Cai, J., Murphy, T.J., and Jones, D.P. (2002). Overexpressed human mitochondrial thioredoxin confers resistance to oxidant-induced apoptosis in human osteosarcoma cells. J. Biol. Chem. *277*, 33242–33248.

Crompton, M. (1999). The mitochondrial permeability transition pore and its role in cell death. Biochem. J. *341*, 233–249.

Crompton, M., Ellinger, H., and Costi, A. (1988). Inhibition by cyclosporin A of a Ca^{2+}-dependent pore in heart mitochondria activated by inorganic phosphate and oxidative stress. Biochem. J. *255*, 357–360.

Davis, W., Ronai, Z., and Tew, K.D. (2001). Cellular thiols and reactive oxygen species in drug-induced apoptosis. J. Pharmacol. Exp. Ther. *296*, 1–6.

Defilippi, P., Retta, S.F., Olivo, C., Palmieri, M., Venturino, M., Silengo, L.,

and Tarone, G. (1995). p125FAK tyrosine phosphorylation and focal adhesion assembly: studies with phosphotyrosine phosphatase inhibitors. Exp. Cell Res. *221*, 141–152.

Doerner, A., Pauschinger, M., Badorff, A., Noutsias, M., Giessen, S., Schulze, K., Bilger, J., Rauch, U., and Schultheiss, H.P. (1997). Tissue-specific transcription pattern of the adenine nucleotide translocase isoforms in humans. FEBS Lett. *414*, 258–262.

Donoghue, N., Yam, P.T.W., Jiang, X., and Hogg, P.J. (2000). Presence of closely spaced protein thiols on the surface of mammalian cells. Protein Sci. *9*, 2436–2445.

Fantin, V.R., Berardi, M.J., Scorrano, L., Korsmeyer, S.J., and Leder, P. (2002). A novel mitochondriotoxic small molecule that selectively inhibits tumor cell growth. Cancer Cell *2*, 29–42.

Folkman, J. (1985). Angiogenesis and its inhibitors. In Important Advances in Oncology, V.T. DeVita, S. Hellman, and S. Rosenberg, eds. (Philadelphia: J.B. Lippincott Company), pp. 42–62.

Gavrieli, Y., Sherman, Y., and Ben-Sasson, S.A. (1992). Identification of programmed cell death in situ via specific labelling of nuclear DNA fragmentation. J. Cell Biol. *119*, 493–501.

Gladyshev, V.N., Liu, A., Novoselov, S.V., Krysan, K., Sun, Q.A., Kryukov, V.M., Kryukov, G.V., and Lou, M.F. (2001). Identification and characterization of a new mammalian glutaredoxin (thioltransferase), Grx2. J. Biol. Chem. *276*, 30374–30380.

Green, D.R., and Evan, G.I. (2002). A matter of life and death. Cancer Cell *1*, 19–30.

Halestrap, A.P., McStay, G.P., and Clarke, S.J. (2002). The permeability transition pore complex: another view. Biochimie *84*, 153–166.

Halestrap, A.P., Woodfield, K.Y., and Connern, C.P. (1997). Oxidative stress, thiol reagents, and membrane potential modulate the mitochondrial permeability transition by affecting nucleotide binding to the adenine nucleotide translocase. J. Biol. Chem. *272*, 3346–3354.

Hanahan, D., and Folkman, J. (1996). Patterns and emerging mechanisms of the angiogenic switch during tumorigenesis. Cell *86*, 353–364.

Haworth, R.A., and Hunter, D.R. (1979). The Ca^{2+}-induced membrane transition in mitochondria. II. Nature of the Ca^{2+} trigger site. Arch. Biochem. Biophys. *195*, 460–467.

Haworth, R.A., and Hunter, D.R. (2000). Control of the mitochondrial permeability transition pore by high-affinity ADP binding at the ADP/ATP translocase in permeabilized mitochondria. J. Bioenerg. Biomembr. *32*, 91–96.

Hiura, T.S., Li, N., Kaplan, R., Horwitz, M., Seagrave, J.C., and Nel, A.E. (2000). The role of a mitochondrial pathway in the induction of apoptosis by chemicals extracted from diesel exhaust particles. J. Immunol. *165*, 2703–2711.

Hoek, J.B., Farber, J.L., Thomas, A.P., and Wang, X. (1995). Calcium ion-dependent signalling and mitochondrial dysfunction: mitochondrial calcium uptake during hormonal stimulation in intact liver cells and its implication for the mitochondrial permeability transition. Biochim. Biophys. Acta *1271*, 93–102.

Holmgren, L., O'Reilly, M.S., and Folkman, J. (1995). Dormancy of micrometastases: balanced proliferation and apoptosis in the presence of angiogenesis suppression. Nat. Med. *1*, 149–153.

Hunter, D.R., and Haworth, R.A. (1979). The Ca^{2+}-induced membrane transition in mitochondria. I. The protective mechanisms. Arch. Biochem. Biophys. *195*, 453–459.

Jackson, C.J., Garbett, P.K., Nissen, B., and Schreiber, L.J. (1990). Binding of human endothelium to Ulex europaeus I-coated Dynabeads: application to the isolation of microvascular endothelium. J. Cell Sci. *96*, 257–262.

Klingenberg, M., and Nelson, D.R. (1994). Structure-function relationships of the ADP/ATP carrier. Biochim. Biophys. Acta *1187*, 241–244.

Ku, D.H., Kagan, J., Chen, S.T., Chang, C.D., Baserga, R., and Wurzel, J. (1990). The human fibroblast adenine nucleotide translocator gene. Molecular cloning and sequencing. J. Biol. Chem. *265*, 16060–16063.

Larochette, N., Decaudin, D., Jacotot, E., Brenner, C., Marzo, I., Susin, S.A., Zamzami, N., Xie, Z., Reed, J., and Kroemer, G. (1999). Arsenite induces apoptosis via a direct effect on the mitochondrial permeability transition pore. Exp. Cell Res. *249*, 413–421.

Lenartowicz, E., Bernardi, P., and Azzone, G.F. (1991). Phenylarsine oxide induces the cyclosporin-A-sensitive membrane permeability transition in rat liver mitochondria. J. Bioenerg. Biomembr. *23*, 679–688.

LeQuoc, K., and LeQuoc, D. (1988). Involvement of the ADP/ATP carrier in calcium-induced perturbations of the mitochondrial inner membrane permeability: importance of the orientation of the nucleotide binding site. Arch. Biochem. Biophys. *265*, 249–257.

Liao, K., Hoffman, R.D., and Lane, M.D. (1991). Phosphotyrosyl turnover in insulin signaling. J. Biol. Chem. *266*, 6544–6553.

Majima, E., Yamaguchi, N., Chuman, H., Shinohara, Y., Ishida, M., Goto, S., and Terada, H. (1998). Binding of the fluorescein derivative eosin Y to the mitochondrial ADP/ATP carrier: characterization of the adenine nucleotide binding site. Biochemistry *37*, 424–432.

McStay, G.P., Clarke, S.J., and Halestrap, A.P. (2002). Role ANT thiol groups in MPTP function. Biochem. J. *367*, 541–548.

Montesano, R., Pepper, M.S., Belin, D., Vassalli, J.D., and Orci, L. (1988). Induction of angiogenesis in vitro by vanadate, and inhibitor of phosphotyrosine phosphatases. J. Cell. Physiol. *134*, 460–466.

Nguyen, M., Shing, Y., and Folkman, J. (1994). Quantitation of angiogenesis and antiangiogenesis in the chick embryo chorioallantoic membrane. Microvasc. Res. *47*, 31–40.

Ochi, T. (1997). Arsenic compound induced increases in glutathione levels in cultured Chinese hamster V79 cells and mechanisms associated with changes in γ-glutamylcysteine synthetase activity, cystine uptake and utilization of cysteine. Arch. Toxicol. *71*, 730–740.

Oliver, M.H., Harrison, N.K., Bishop, J.E., Cole, P.J., and Laurent, G.J. (1989). A rapid and convenient assay for counting cells cultured in microwell plates: application for assessment of growth factors. J. Cell Sci. *92*, 513–518.

O'Reilly, M.S., Boehm, T., Shing, Y., Fukai, N., Vasios, G., Lane, W.S., Flynn, E., Birkhead, J.R., Olsen, B.R., and Folkman, J. (1997). Endostatin: an endogenous inhibitor of angiogenesis and tumor growth. Cell *88*, 277–285.

Papa, S. (1996). Mitochondrial oxidative phosphorylation changes in the life span. Molecular aspects and physiopathological implications. Biochim. Biophys. Acta *1276*, 87–105.

Pedersen, P.L. (1978). Tumor mitochondria and the bioenergetics of cancer cells. Prog. Exp. Tumor Res. *22*, 190–274.

Petit, J.M., Maftah, A., Ratinaud, M.H., and Julien, R. (1992). 10N-nonyl acridine orange interacts with cardiolipin and allows the quantification of this phospholipid in isolated mitochondria. Eur. J. Biochem. *209*, 267–273.

Poot, M., Zhang, Y.Z., Kramer, J.A., Wells, K.S., Jones, L.J., Hanzel, D.K., Lugade, A.G., Singer, V.L., and Haugland, R.P. (1996). Analysis of mitochondrial morphology and function with novel fixable fluorescent stains. J. Histochem. Cytochem. *44*, 1363–1372.

Powis, G., and Montfort, W.R. (2001). Properties and biological activities of thioredoxins. Annu. Rev. Pharmacol. Toxicol. *41*, 261–295.

Radabaugh, T.R., and Aposhian, H.V. (2000). Enzymatic reduction of arsenic compounds in mammalian systems: reduction of arsenate to arsenite by human liver arsenate reductase. Chem. Res. Toxicol. *13*, 26–30.

Raha, S., and Robinson, B.H. (2000). Mitochondria, oxygen free radicals, disease and ageing. Trends Biochem. Sci. *25*, 502–508.

Rizzuto, R., Bernardi, P., and Pozzan, T. (2000). Mitochondria as all-round players of the calcium game. J. Physiol. *529*, 37–47.

Schnaitman, C., and Greenawalt, J.W. (1968). Enzymatic properties of the inner and outer membranes of rat liver mitochondria. J. Cell Biol. *38*, 158–175.

Schuliga, M., Chouchane, S., and Snow, E.T. (2002). Upregulation of glutathione-regulated genes and enzyme activities in cultured human cells by sublethal concentrations of inorganic arsenic. Toxicol. Sci. *70*, 183–192.

Smiley, S.T., Reers, M., Mottola-Hartshorn, C., Lin, M., Chen, A., Smith, T.W., Steele, G.D., Jr., and Chen, L.B. (1991). Intracellular heterogeneity in mitochondrial membrane potentials revealed by a J-aggregate-forming lipophilic cation JC-1. Proc. Natl. Acad. Sci. USA *88*, 3671–3675.

Soeda, S., Shimada, T., Koyanagi, S., Yokomatsu, T., Murano, T., Shibuya, S., and Shimeno, H. (2002). An attempt to promote neo-vascularization by employing a newly synthesized inhibitor of protein tyrosine phosphatases. FEBS Lett. *524*, 54–58.

Turrens, J.F., and Boveris, A. (1980). Generation of superoxide anion by the NADH dehydrogenase of bovine heart mitochondria. Biochem. J. *191*, 421–427.

Vanden Hoek, T.L., Becker, L.B., Shao, Z., Li, C., and Schumacker, P.T. (1998). Reactive oxygen species released from mitochondria during brief hypoxia induce preconditioning in cardiomyocytes. J. Biol. Chem. *29*, 18092–18098.

Weidner, N., Semple, J.P., Welch, W.R., and Folkman, J. (1991). Tumor angiogenesis and metastasis–correlation in invasive breast carcinoma. N. Engl. J. Med. *324*, 1–8.

Yuan, Y., Meng, F.Y., Huang, Q., Hawker, J., and Wu, H.M. (1998). Tyrosine phosphorylation of paxillin/pp125FAK and microvascular endothelial barrier function. Am. J. Physiol. *275*, H84–H93.

Zanetti, M., Zwacka, R.M., Engelhardt, J.F., Katusic, Z.S., and O'Brien, T. (2001). Superoxide anions and endothelial cell proliferation in normoglycemia and hyperglycemia. Arterioscler. Thromb. Vasc. Biol. *21*, 195–200.